



# Individual and interactive effects of warming and CO<sub>2</sub> on *Pseudo-nitzschia subcurvata* and *Phaeocystis antarctica*, two dominant phytoplankton from the Ross Sea, Antarctica

Zhi Zhu, Pingping Qu, Jasmine Gale, Feixue Fu, and David A. Hutchins

Department of Biological Science, University of Southern California, Los Angeles, CA 90089, USA

Correspondence to: David A. Hutchins (dahutch@usc.edu)

Received: 24 January 2017 – Discussion started: 3 February 2017

Revised: 3 October 2017 – Accepted: 7 October 2017 – Published: 29 November 2017

**Abstract.** We investigated the effects of temperature and CO<sub>2</sub> variation on the growth and elemental composition of cultures of the diatom *Pseudo-nitzschia subcurvata* and the prymnesiophyte *Phaeocystis antarctica*, two ecologically dominant phytoplankton species isolated from the Ross Sea, Antarctica. To obtain thermal functional response curves, cultures were grown across a range of temperatures from 0 to 14 °C. In addition, a co-culturing experiment examined the relative abundance of both species at 0 and 6 °C. CO<sub>2</sub> functional response curves were conducted from 100 to 1730 ppm at 2 and 8 °C to test for interactive effects between the two variables. The growth of both phytoplankton was significantly affected by temperature increase, but with different trends. Growth rates of *P. subcurvata* increased with temperature from 0 °C to maximum levels at 8 °C, while the growth rates of *P. antarctica* only increased from 0 to 2 °C. The maximum thermal limits of *P. subcurvata* and *P. antarctica* where growth stopped completely were 14 and 10 °C, respectively. Although *P. subcurvata* outgrew *P. antarctica* at both temperatures in the co-incubation experiment, this happened much faster at 6 than at 0 °C. For *P. subcurvata*, there was a significant interactive effect in which the warmer temperature decreased the CO<sub>2</sub> half-saturation constant for growth, but this was not the case for *P. antarctica*. The growth rates of both species increased with CO<sub>2</sub> increases up to 425 ppm, and in contrast to significant effects of temperature, the effects of CO<sub>2</sub> increase on their elemental composition were minimal. Our results suggest that future warming may be more favorable to the diatom than to the prymnesiophyte, while CO<sub>2</sub> increases may not be a major factor in future competitive interactions between *Pseudo-nitzschia subcurvata* and *Phaeocystis antarctica* in the Ross Sea.

## 1 Introduction

Global temperature is predicted to increase 2.6 to 4.8 °C by 2100 with increasing anthropogenic CO<sub>2</sub> emissions (IPCC, 2014). The temperature of the Southern Ocean has increased even faster than global average temperature (Meredith and King, 2005), and predicted future climate warming may profoundly change the ocean carbon cycle in this region (Sarmiento et al., 1998). The Ross Sea, Antarctica, is one of the most productive area in the ocean, and features annual austral spring and summer algal blooms dominated by *Phaeocystis* and diatoms that contribute as much as 30 % of total primary production in the Southern Ocean (Arrigo et al., 1999, 2008; Smith et al., 2000, 2014a). The responses of phytoplankton in the Ross Sea to future temperature change (Rose et al., 2009; Xu et al., 2014; Zhu et al., 2016) in combination with intensified stratification (Sarmiento et al., 1998) could lead to intensified future diatom blooms (Smith et al., 2014b), and the physiological effects of warming may partially compensate for a lack of iron throughout much of this region (Hutchins and Boyd, 2016).

In the Ross Sea, the colonial prymnesiophyte *Phaeocystis antarctica* typically blooms in austral spring and early summer, and diatoms including *Pseudo-nitzschia subcurvata* and *Chaetoceros* spp. bloom later in the austral summer (Arrigo et al., 1999, 2000; DiTullio and Smith, 1996; Goffart et al., 2000; Rose et al., 2009). Both diatoms and *P. antarctica* play an important role in anthropogenic CO<sub>2</sub> drawdown and the global carbon cycle; additionally, they contribute significantly to the global silicon and sulfur cycles, respectively (Arrigo et al., 1999; Tréguer et al., 1995; Schoemann et al., 2005). Furthermore, the N:P and C:P ratios of *P. antarctica*

*tica* are higher than those of diatoms, and thus they contribute unequally to the carbon, nitrogen, and phosphorus cycles (Arrigo et al., 1999, 2000). Diatoms are preferred by many planktonic herbivores over *P. antarctica*, and so the two groups also differentially influence the food webs of the Southern Ocean (Knox, 1994; Caron et al., 2000; Haberman et al., 2003).

Arrigo et al. (1999) suggested that the spatial and temporal distributions of *P. antarctica* and diatoms in the Ross Sea are determined by the mixed layer depth, while Liu and Smith (2012) indicated that temperature is more important in shaping the distribution of these two dominant groups of phytoplankton. Smith and Jones (2015) presented evidence for the importance of deep mixing and the critical depth for the timing of transitions from *P. antarctica* to diatom blooms. Zhu et al. (2016) observed that a 4 °C temperature increase promoted the growth rates of several dominant diatoms isolated from the Ross Sea, including *P. subcurvata*, *Chaetoceros* sp., and *Fragilariopsis cylindrus*, but not the growth rates of *P. antarctica*. In addition, both field and laboratory research has suggested that temperature increase and iron addition can synergistically promote the growth of Ross Sea diatoms (Rose et al., 2009; Zhu et al., 2016; Hutchins and Boyd, 2016). Thus, it is possible that phytoplankton community structure in this region may change in the future under a global warming scenario.

In addition to temperature increases, ocean uptake of 30 % of total emitted anthropogenic CO<sub>2</sub> has led to a 0.1 pH unit decrease in surface water, corresponding to a 26 % increase in acidity (IPCC, 2014). The global CO<sub>2</sub> concentration is predicted to increase to around 800 ppm by 2100, which will lead to a further decrease in surface seawater pH of 0.3–0.4 units (Orr et al., 2005; IPCC, 2014). CO<sub>2</sub> increases have been found to promote the growth and affect the physiology of many but not all phytoplankton species tested (Fu et al., 2007, 2008; King et al., 2011; Xu et al., 2014; Hutchins and Fu 2017).

Research on the effects of CO<sub>2</sub> increases on *Phaeocystis antarctica* and Antarctic diatoms is still scarce. Xu et al. (2014) suggested that future conditions (higher temperature, CO<sub>2</sub>, and irradiance) may shift phytoplankton community structure towards diatoms and away from *P. antarctica* in the Ross Sea. Trimborn et al. (2013) discovered that the growth rates of *P. antarctica* and *P. subcurvata* were not significantly promoted by high CO<sub>2</sub> relative to ambient CO<sub>2</sub> at 3 °C. In contrast, Wang et al. (2010) observed that the growth rates of the closely related temperate colonial species *Phaeocystis globosa* increased significantly at 750 ppm CO<sub>2</sub> relative to 380 ppm CO<sub>2</sub>.

Many studies have shown that primary production in various parts of the Southern Ocean is limited by iron supply (Martin et al., 1990; Takeda, 1998; Boyd et al., 2000; Sedwick et al., 2000; Hutchins et al., 2002; Coale et al., 2004), and several have addressed the effects of iron and warming on the growth of phytoplankton from the Ross Sea (Rose et

al., 2009; Zhu et al., 2016; Hutchins and Boyd, 2016). Thus, an important goal of phytoplankton research is to also gain an understanding of how global warming together with ocean acidification may shift the phytoplankton community in the Ross Sea (Arrigo et al., 1999; DiTullio et al., 2000). This study aimed to explore the effects of increases in temperature and CO<sub>2</sub> availability, both individually and in combination, on *P. antarctica* and *P. subcurvata* isolated from the Ross Sea, Antarctica. These results may shed light on the potential effects of global change on the marine ecosystem and the cycles of carbon and nutrients in the highly productive coastal polynyas of Antarctica.

## 2 Materials and methods

### 2.1 Strains and growth conditions

*P. subcurvata* and *P. antarctica* were isolated from the ice edge in McMurdo Sound (77.62° S, 165.47° E) in the Ross Sea, Antarctica, during January 2015; *P. antarctica* cultures grew as small colonies (~4–12 cells) in all the experiments. All stock cultures were grown in Aquil medium (100 μmol L<sup>-1</sup> NO<sub>3</sub><sup>-</sup>, 100 μmol L<sup>-1</sup> SiO<sub>4</sub><sup>4-</sup>, 10 μmol L<sup>-1</sup> PO<sub>4</sub><sup>3-</sup>) made with 0.2 μM-filtered seawater that was collected from the same Ross Sea locale as the culture isolates (Sunda et al., 2005). Stock and experimental cultures were grown in Fe-replete Aquil medium (0.5 μM). Although phytoplankton in the open Ross Sea polynya are generally proximately iron-limited (Ryan-Keogh et al., 2017), these culture conditions are relevant to the coastal McMurdo Sound ice edge environment in the early spring when Fe is relatively abundant, and typically not limiting. This “winter reserve” iron is then drawn down in this nearshore environment over the course of the seasonal algal bloom to eventually reach limiting levels (Sedwick et al., 2011; Bertrand et al., 2015). Our experiments address warming and acidification responses in *P. subcurvata* and *P. antarctica* in the absence of any differential effects of Fe availability; interactive effects of Fe limitation with warming and/or acidification in these two species are presented in Xu et al. (2014) and Zhu et al. (2016). Cultures were maintained at 0 °C in a walk-in incubator under 24 h cold white fluorescence light (80 μmol photons m<sup>-2</sup> s<sup>-1</sup>).

### 2.2 Experimental design

For thermal functional response curves, experimental cultures of both phytoplankton were grown in triplicate 500 mL acid-washed polycarbonate bottles and gradually acclimated by a series of step-wise transfers to a range of temperatures, including 0, 2, 4, 6, 8, and 10 °C (*P. antarctica* died at 10 °C) under the same light cycle as stock cultures. Cultures were diluted semi-continuously following Zhu et al. (2016), allowing them to be maintained in continuous exponential growth

and so facilitating comparisons between treatments in the same physiological growth stage. All of the cultures were acclimated to their respective temperatures for 8 weeks before the commencement of the experiment. At this point, after the growth rates were verified to be stable for at least three to five consecutive transfers, the cultures were sampled 48 h after dilution (Zhu et al., 2016).

For CO<sub>2</sub> functional response curves, *P. antarctica* and *P. subcurvata* were also grown in triplicate in a series of six CO<sub>2</sub> concentrations from ~100 to ~1730 ppm in triplicate 500 mL acid-washed polycarbonate bottles at both 2 and 8 °C using same dilution technique as above. The CO<sub>2</sub> concentration was achieved by gently bubbling with 0.2 µm filtered air–CO<sub>2</sub> mixture (Gilmore, CA) and carbonate system equilibration was ensured by pH and dissolved inorganic carbon (DIC) measurements (King et al., 2015; see below).

An additional experiment tested whether temperature-related trends in growth rates observed in monocultures were maintained when both species were grown together in a simple model community. For this examination of thermal effects on the growth of *P. antarctica* and *P. subcurvata* in co-culture (pre-acclimated to respective temperatures), the isolates were mixed at equal Chl *a* (chlorophyll *a*) concentrations and grown together for 6 days in triplicate bottles at both 0 and 6 °C. These temperatures chosen to span the optimum growth ranges of both species (see Results, below). The relative abundance of each phytoplankton was then calculated based on cell counts taken on days 0, 3, and 6.

### 2.3 Growth rates

Cell count samples were counted on a Sedgewick Rafter Grid using an Olympus BX51 microscope before and after dilution for each treatment. Samples that could not be counted immediately were preserved with Lugol's iodine solution (final concentration 2 %) and stored at 4 °C until counting. Specific growth rates (d<sup>-1</sup>) were calculated following Eq. (1):

$$\mu = (\ln N_1 - \ln N_0)/t, \quad (1)$$

where  $N_0$  and  $N_1$  are the cell density at the beginning and end of a dilution period, respectively, and  $t$  is the duration of the dilution period (Zhu et al., 2016). The  $Q_{10}$  of growth rates was calculated following Chauvi-Berlinck et al. (2002) as Eq. (2):

$$Q_{10} = (\mu_2/\mu_1)^{10/(T_2-T_1)}, \quad (2)$$

where  $\mu_1$  and  $\mu_2$  are the specific growth rates of the phytoplankton at temperatures  $T_1$  and  $T_2$ , respectively. The growth rates were fitted to Eq. (3) to estimate the thermal reaction norms of each species:

$$f(T) = ae^{bT} (1 - ((T - z)/(w/2))^2), \quad (3)$$

where specific growth rate  $f$  depends on temperature ( $T$ ) and temperature niche width ( $w$ ), and other empirical parameters

$z$ ,  $a$ , and  $b$  were estimated by maximum likelihood (Thomas et al., 2012; Boyd et al., 2013). Afterwards, the optimum temperature for growth and maximum growth rate were estimated by numerically maximizing the equation (Boyd et al., 2013). The growth rates of all the species at all the CO<sub>2</sub> levels were fitted to Michaelis–Menten equation as Eq. (4),

$$\mu = \mu_{\max} S / (K_{1/2} + S), \quad (4)$$

to estimate maximum growth rates ( $\mu_{\max}$ ) and half-saturation constants ( $K_{1/2}$ ) for CO<sub>2</sub> concentration ( $S$ ). In the CO<sub>2</sub> curve experiments growth rates for both these autotrophic species were assumed to be zero at 0 ppm CO<sub>2</sub>, and in the thermal curve experiments growth rates were assumed to be zero at –2 °C, approximately the freezing point of seawater.

### 2.4 Elemental and Chl *a* analysis

Culture samples for particulate organic carbon/nitrogen (POC/PON) and particulate organic phosphorus (POP) analyses were filtered onto pre-combusted (500 °C for 2 h) GF/F filters and dried at 60 °C overnight. A 30 mL aliquot of *P. subcurvata* culture for each treatment was filtered onto 2 µm polycarbonate filters (GE Healthcare, CA) and dried in an oven at 60 °C overnight for biogenic silica (BSi) analysis. The analysis method of POC/PON and POP followed Fu et al. (2007), and BSi analysis followed Paasche et al. (1973). An aliquot of 30 to 50 mL from each treatment replicate was filtered onto GF/F filters and extracted with 90 % acetone at –20 °C for 24 h for Chl *a* analysis. The Chl *a* concentration was then determined using the non-acidification method on a 10AU<sup>TM</sup> fluorometer (Turner Design, CA) (Fu et al., 2007).

### 2.5 pH and dissolved inorganic carbon (DIC) measurements

pH was measured using a pH meter (Thermo Scientific, MA), calibrated with pH 7 and 10 buffer solutions. For DIC analyses, an aliquot of 25 mL was preserved with 200 µL 5 % HgCl<sub>2</sub> and stored in the dark at 4 °C until analysis. Total DIC was measured using a CM140 total inorganic carbon analyzer (UIC Inc., IL). An aliquot of 5 mL sample was injected into the sparging column of acidification unit CM5230 (UIC Inc., IL) followed by 2 mL 10 % phosphoric acid. Flow-rate-controlled pure nitrogen was used as the carrier gas, and the CO<sub>2</sub> released from the DIC pool in the sample was quantified with a CM5015 CO<sub>2</sub> coulometer (UIC Inc., IL) using absolute coulometric titration. The carbonate buffer system was sampled for each of the triplicate bottles in each treatment at the beginning and end of the experiments; reported values are final ones. The  $p\text{CO}_2$  in growth media was calculated using CO2SYS (Pierrot et al., 2006). These carbonate system measurements are shown in Table 1, along with the corresponding calculated  $p\text{CO}_2$  values calculated. Kinetic parameters were calculated using the individual calculated  $p\text{CO}_2$  values

**Table 1.** The measured pH and dissolved inorganic carbon (DIC) as well as calculated  $p\text{CO}_2$  of *P. subcurvata* and *P. antarctica* at 2 and 8 °C in each treatment. Values represent the means and errors are the standard deviations of triplicate bottles.

<i>P. subcurvata</i>		<i>P. antarctica</i>	
2 °C	8 °C	2 °C	8 °C
<b>pH</b>			
8.36 ± 0.04	8.51 ± 0.04	8.40 ± 0.03	8.45 ± 0.03
8.25 ± 0.04	8.36 ± 0.01	8.22 ± 0.04	8.29 ± 0.01
8.07 ± 0.01	8.17 ± 0.01	8.09 ± 0.02	8.14 ± 0.00
7.86 ± 0.02	7.99 ± 0.01	7.85 ± 0.01	7.94 ± 0.00
7.68 ± 0.01	7.79 ± 0.02	7.65 ± 0.01	7.75 ± 0.00
7.35 ± 0.01	7.46 ± 0.02	7.34 ± 0.01	7.45 ± 0.00
<b>DIC (<math>\mu\text{mol kg}^{-1}</math>)</b>			
1890.1 ± 26.6	1846.5 ± 15.8	1847.1 ± 30.0	1831.1 ± 22.7
2049.1 ± 10.8	1985.7 ± 2.1	2033.9 ± 15.0	2014.2 ± 19.9
2131.3 ± 9.4	2067.5 ± 4.7	2136.6 ± 5.6	2085.3 ± 15.3
2190.4 ± 2.8	2156.1 ± 13.9	2168.1 ± 12.4	2167.4 ± 21.5
2260.0 ± 22.2	2234.8 ± 10.3	2252.1 ± 11.5	2238.7 ± 12.0
2340.1 ± 19.4	2334.5 ± 18.8	2338.2 ± 12.1	2323.7 ± 11.5
<b><math>p\text{CO}_2</math> (ppm)</b>			
109.1 ± 9.3	94.4 ± 10.1	96.6 ± 9.5	108.8 ± 8.8
158.6 ± 15.5	150.3 ± 3.6	171.2 ± 14.4	183.6 ± 4.2
263.1 ± 5.9	254.2 ± 9.9	246.4 ± 9.9	280.3 ± 0.6
450.2 ± 17.3	414.9 ± 12.0	462.2 ± 12.1	480.9 ± 4.7
740.9 ± 10.6	708.8 ± 23.5	786.9 ± 10.3	784.1 ± 4.8
1751.2 ± 35.9	1675.3 ± 49.4	1769.9 ± 59.5	1720.3 ± 18.3

for each replicate (see above), but for convenience, the  $\text{CO}_2$  treatments are referred to in the text using the mean value of all experimental bottles, rounded to the nearest 5 ppm: these values are 100, 205, 260, 425, 755, and 1730 ppm.

## 2.6 Statistical analysis

All statistical analyses and model fitting, including Student's  $t$  tests, ANOVA, Tukey's HSD test, two-way ANOVA, and thermal reaction norms estimation, were conducted using the open-source statistical software R version 3.1.2 (R Foundation).

## 3 Results

### 3.1 Temperature effects on growth rates

Temperature increase significantly affected the growth rates of both *P. antarctica* and *P. subcurvata*, but with different trends ( $p < 0.05$ ) (Fig. 1). The specific growth rates of *P. subcurvata* increased from 0 to 8 °C ( $p < 0.05$ ) and then significantly decreased at 10 °C ( $p < 0.05$ ) (Fig. 1). The growth rates of *P. antarctica* significantly increased from 0 to 2 °C, plateaued at 4 and 6 °C, and then significantly decreased from 6 to 8 °C ( $p < 0.05$ ) (Fig. 1). *P. antarctica* and *P. subcur-*

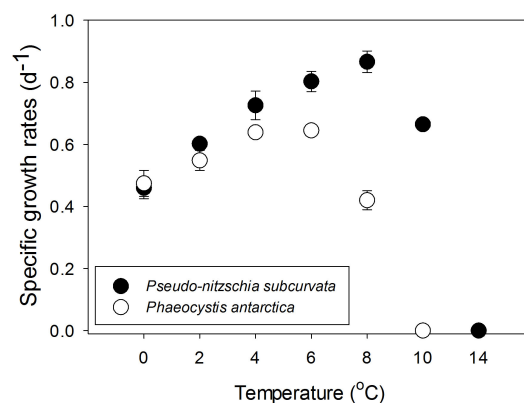


**Figure 1.** Thermal functional response curves showing specific growth rates of *Pseudo-nitzschia subcurvata* and *Phaeocystis antarctica* across a range of temperatures from 0 to 14 °C. Values represent the means and error bars represents the standard deviations of triplicate samples.

*vata* stopped growing at 10 and 14 °C, respectively (Fig. 1). The specific growth rates of *P. subcurvata* were not significantly different from those of *P. antarctica* at 0, 2, and 4 °C, but they became significantly higher than *P. antarctica* at 6 °C and remained significantly higher than *P. antarctica*

**Table 2.** Statistical comparison of the results for each of the three thermal traits: optimum temperature ( $^{\circ}\text{C}$ ), maximum growth rate ( $\text{d}^{-1}$ ), and temperature niche width (W)\* of *P. subcurvata* and *P. antarctica*.

Species	Optimum temperature ( $^{\circ}\text{C}$ )	Maximum growth rates ( $\text{d}^{-1}$ )	W upper CI	W lower CI	$Q_{10}$
<i>P. subcurvata</i>	7.36	0.86	12.19	$\leq 2.0$	3.17
<i>P. antarctica</i>	4.85	0.66	9.52	$\leq 2.0$	2.11

\* The statistical results for the lower bound of temperate niche width in both species were lower than  $-2.0^{\circ}\text{C}$ , the freezing point of seawater.

through 8 and  $10^{\circ}\text{C}$  ( $p < 0.05$ ) (Fig. 1). The optimum temperatures for growth of *P. antarctica* and *P. subcurvata* were 4.85 and  $7.36^{\circ}\text{C}$ , respectively, both well above the current temperature in the Ross Sea, Antarctica (Table 2). In addition, the estimated temperature niche width of *P. subcurvata* ( $-2$ – $12.19^{\circ}\text{C}$ ) is wider than that of *P. antarctica* ( $-2.0$  to  $9.52^{\circ}\text{C}$ ) (Table 2); calculated minimum temperatures estimated from the thermal niche width equation were less than  $-2.0^{\circ}$ , the freezing point of seawater, and so growth is assumed to terminate at  $-2.0^{\circ}$ . The  $Q_{10}$  value of the growth rate of *P. antarctica* from 0 to  $4^{\circ}\text{C}$  is 2.11, which is lower than the  $Q_{10}$  value of 3.17 for *P. subcurvata* over the same temperature interval ( $p < 0.05$ ) (Table 2).

### 3.2 Temperature effects on elemental composition

The C : N and N : P ratios of *P. subcurvata* were unaffected by changing temperature (Fig. 2a, b), but the C : P, C : Si, and C : Chl *a* ratios of this species were significantly affected ( $p < 0.05$ ) (Fig. 2c, d, Fig. 3). The C : P ratios of *P. subcurvata* were slightly but significantly lower in the middle of the tested temperature range. They were higher at 8 and  $10^{\circ}\text{C}$  than at 2, 4, and  $6^{\circ}\text{C}$  ( $p < 0.05$ ) (Fig. 2c), and also significantly higher at  $10^{\circ}\text{C}$  than at  $0^{\circ}\text{C}$  (Fig. 2c). The C : Si ratios of *P. subcurvata* showed a similar pattern of slightly lower values at mid-range temperatures; at 0 and  $2^{\circ}\text{C}$  they were significantly higher than at 6 and  $8^{\circ}\text{C}$  ( $p < 0.05$ ) (Fig. 2d), and significantly higher at 2 and  $10^{\circ}\text{C}$  than at 4 and  $8^{\circ}\text{C}$ , respectively (Fig. 2d). The C : Chl *a* ratios of *P. subcurvata* also showed this trend of somewhat lower values in the middle of the thermal gradient. At 0, 8 and  $10^{\circ}\text{C}$ , C : Chl *a* ratios were significantly higher than at 2, 4, and  $6^{\circ}\text{C}$  ( $p < 0.05$ ), and also significantly higher at  $10^{\circ}\text{C}$  than at 0 and  $8^{\circ}\text{C}$  (Fig. 3).

The C : N, N : P, C : P, and C : Chl *a* ratios of *P. antarctica* were not significantly different across the temperature range (Figs. 2a, b, c, 3). The N : P ratios of *P. antarctica* were significantly higher than those of *P. subcurvata* at 2, 6, and  $8^{\circ}\text{C}$  ( $p < 0.05$ ) (Fig. 2b). Additionally, the C : P ratios of *P. antarctica* were significantly higher than those of *P. subcurvata* at 6 and  $8^{\circ}\text{C}$  ( $p < 0.05$ ) (Fig. 2c), and the C : Chl *a* ratios of *P. antarctica* were significantly higher than values of *P. subcurvata* at all the temperatures tested ( $p < 0.05$ ) (Fig. 3).

Temperature change significantly affected the quotas of cellular carbon (C), cellular nitrogen (N), cellular phospho-

rus (P), cellular silica (Si), and cellular Chl *a* of *P. subcurvata* ( $p < 0.05$ ) (Table 3). The cellular C and N quotas of *P. subcurvata* were significantly higher at  $8^{\circ}\text{C}$  than at  $0^{\circ}\text{C}$  ( $p < 0.05$ ) (Table 3), the cellular P quotas of *P. subcurvata* were significantly higher at  $4^{\circ}\text{C}$  than at 0, 2, and  $10^{\circ}\text{C}$  ( $p < 0.05$ ) (Table 3), and the cellular Si quotas of *P. subcurvata* were significantly higher at  $8^{\circ}\text{C}$  than at 0 and  $2^{\circ}\text{C}$ . Si quotas were also significantly higher at 4 and  $6^{\circ}\text{C}$  than at  $0^{\circ}\text{C}$  ( $p < 0.05$ ) (Table 3). The extreme temperatures significantly decreased the cellular Chl *a* quotas of *P. subcurvata*, as the cellular Chl *a* quotas of this species were significantly higher at 4, 6, and  $8^{\circ}\text{C}$  than at 0 and  $10^{\circ}\text{C}$  ( $p < 0.05$ ) (Table 3).

Temperature change significantly affected the cellular P quotas and cellular Chl *a* quotas of *P. antarctica* ( $p < 0.05$ ), but not the cellular C and N quotas ( $p > 0.05$ ) (Table 3). The cellular P quotas of *P. antarctica* were significantly higher at  $0^{\circ}\text{C}$  than at  $8^{\circ}\text{C}$  ( $p < 0.05$ ) (Table 3), and the Chl *a* quotas of the prymnesiophyte were significantly lower at  $8^{\circ}\text{C}$  than at 0, 2, and  $6^{\circ}\text{C}$  ( $p < 0.05$ ) (Table 3).

### 3.3 Co-incubation at two temperatures

A warmer temperature favored the dominance of *P. subcurvata* over *P. antarctica* in the model community experiment. Although *P. subcurvata* increased its abundance relative to the prymnesiophyte at both temperatures by day 6, this increase was larger and happened much faster at  $6^{\circ}\text{C}$  (from 31 to 72%) relative to  $0^{\circ}\text{C}$  (from 31 to 38%) ( $p < 0.05$ ) (Fig. 4).

### 3.4 $\text{CO}_2$ effects on specific growth rates at two temperatures

The carbonate system was relatively stable across the range of  $\text{CO}_2$  levels during the course of the experiment (Table 1).  $\text{CO}_2$  concentration significantly affected the growth rates of *P. subcurvata* at both temperatures (Fig. 5). The growth rates of the diatom at  $2^{\circ}\text{C}$  increased steadily with  $\text{CO}_2$  concentration increase from 205 to 425 ppm ( $p < 0.05$ ), but were saturated at 755 and 1730 ppm (Fig. 5a). Similarly, the growth rates of *P. subcurvata* at  $8^{\circ}\text{C}$  increased with  $\text{CO}_2$  concentration increase from 205 to 260 ppm ( $p < 0.05$ ), and were saturated at 425, 755 and 1730 ppm (Fig. 5b). The growth rates of the diatom at all  $\text{CO}_2$  concentrations tested at  $8^{\circ}\text{C}$  were significantly higher than at  $2^{\circ}\text{C}$  ( $p < 0.05$ ); for instance,

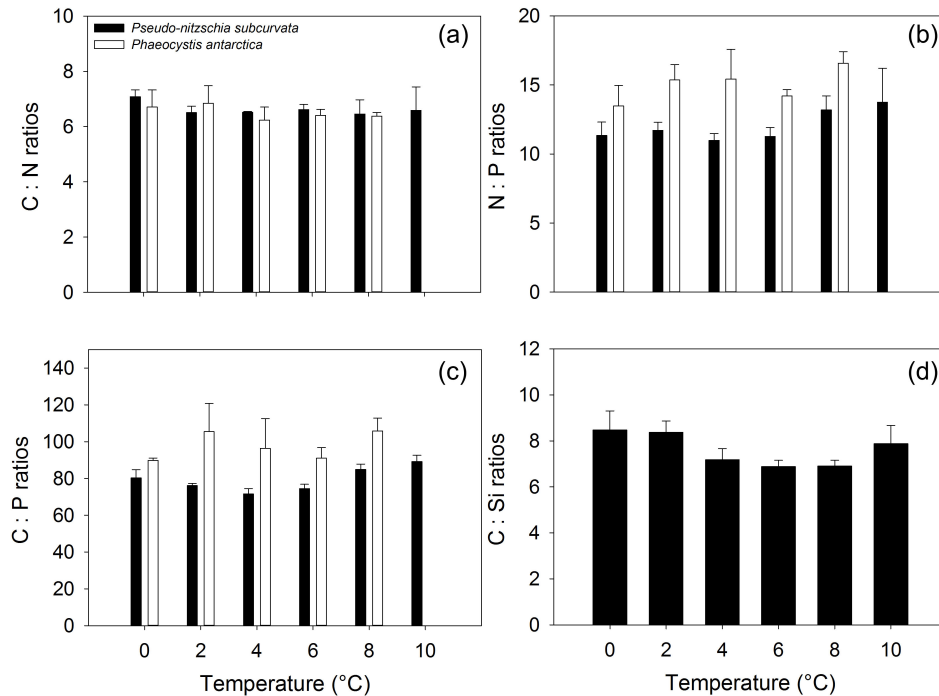


**Figure 2.** The C:N ratios (a), N:P ratios (b), and C:P ratios (c) of *Pseudo-nitzschia subcurvata* and *Phaeocystis antarctica* and (d) the C:Si ratios of *Pseudo-nitzschia subcurvata* from the thermal response curves shown in Fig. 1 for a range of temperatures from 0 to 10°C. Values represent the means and error bars represents the standard deviations of triplicate samples.

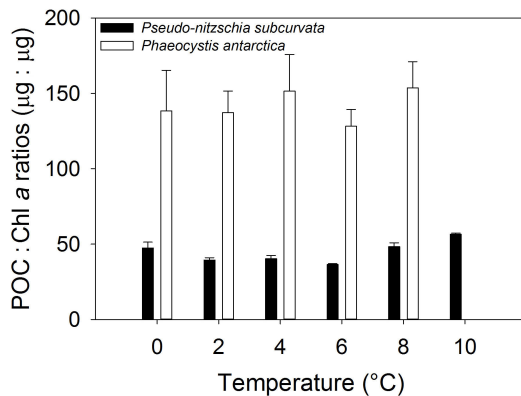


**Figure 3.** The C:Chl *a* ratios of *Pseudo-nitzschia subcurvata* and *Phaeocystis antarctica* from the thermal response curves shown in Fig. 1 for a range of temperatures from 0 to 10°C. Values represent the means and error bars represents the standard deviations of triplicate samples.

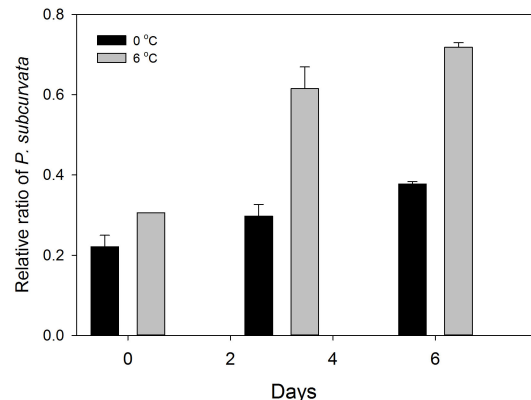


**Figure 4.** The relative abundance of *Pseudo-nitzschia subcurvata* in a 6-day competition experiment with *Phaeocystis antarctica* at 0 and 6°C. The competition experiments were started with equal Chl *a* concentrations for both species, and the relative abundance was calculated based on cell counts. Values represent the means and error bars represents the standard deviations of triplicate samples.

the maximum growth rate of *P. subcurvata* at 8°C was  $0.88 \text{ d}^{-1}$ , significantly higher than the value of  $0.60 \text{ d}^{-1}$  at 2°C ( $p < 0.5$ ) (Table 4). In addition, the  $p\text{CO}_2$  half-saturation constant ( $K_{1/2}$ ) of *P. subcurvata* at 8°C was 10.7 ppm, significantly lower than 66.0 ppm at 2°C ( $p < 0.5$ ) (Table 4). Thus, temperature and  $\text{CO}_2$  concentration increase interactively increased the growth rates of *P. subcurvata* ( $p < 0.05$ ).

$\text{CO}_2$  concentration also significantly affected the growth rates of *P. antarctica* at both 2 and 8°C. The growth rates of the prymnesiophyte at both 2 and 8°C increased with  $\text{CO}_2$  concentration increase from 100 to 260 ppm ( $p < 0.05$ ), and were saturated at 425 and 755 ppm (Fig. 5c, d). The growth rates of *P. antarctica* at 2°C decreased slightly at

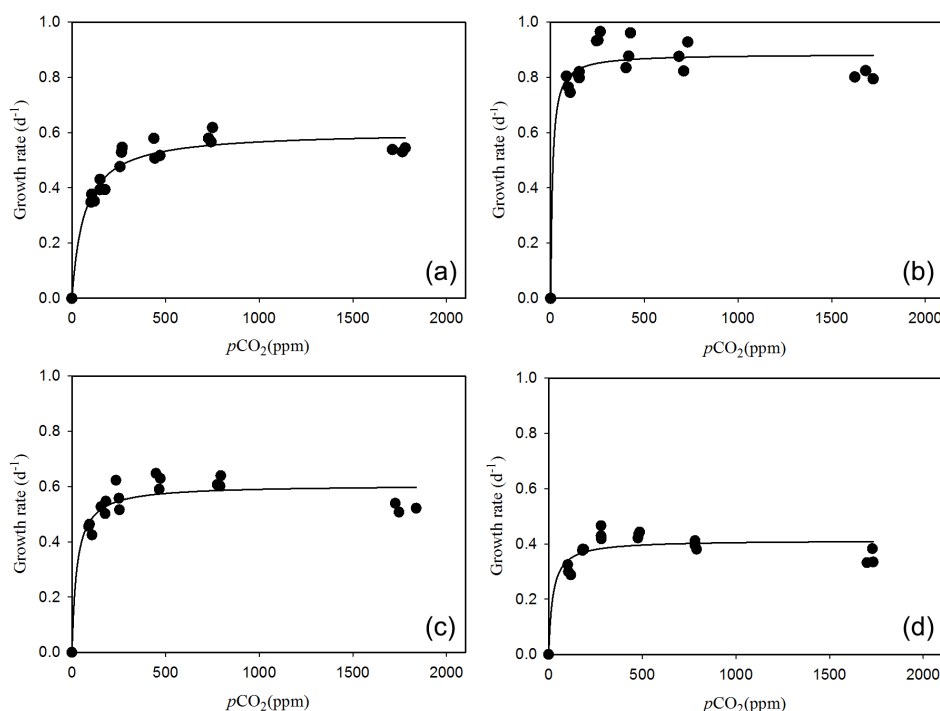


**Figure 5.** CO<sub>2</sub> functional response curves showing specific growth rates (and fitted curves) across a range of CO<sub>2</sub> concentrations from ~100 to ~1730 ppm at 2 and at 8 °C. *Pseudo-nitzschia subcurvata* at 2 °C (a) and 8 °C (b) and *Phaeocystis antarctica* at 2 (c) and 8 °C (d). Values represent the means and error bars represents the standard deviations of triplicate samples.

1730 ppm relative to 425 and 755 ppm ( $p < 0.05$ ) (Fig. 5c). The maximum growth rate of *P. antarctica* at 8 °C was  $0.43 \text{ d}^{-1}$ , significantly lower than the value of  $0.61 \text{ d}^{-1}$  at 2 °C ( $p < 0.05$ ) (Table 4). The  $p\text{CO}_2$  half-saturation constants of *P. antarctica* at 2 and 8 °C were not significantly different (Table 4), and thus no interactive effect of temperature and CO<sub>2</sub> was observed on the growth rate of the prymnesiophyte ( $p > 0.05$ ).

### 3.5 CO<sub>2</sub> effects on elemental composition at two temperatures

CO<sub>2</sub> concentration variation did not affect the C : N, N : P, or C : P ratios of *P. subcurvata* at either 2 or 8 °C. The C : Si ratios of *P. subcurvata* were significantly higher at 1730 ppm relative to lower  $p\text{CO}_2$  levels, except at 755 ppm at 8 °C ( $p < 0.05$ ) (Table 5). The N : P ratios of *P. subcurvata* at 8 °C were significantly higher than at 2 °C at all the CO<sub>2</sub> levels tested except 100 ppm ( $p < 0.05$ ) (Table 5). The C : P ratios of *P. subcurvata* at 8 °C were significantly higher than at 2 °C at all the CO<sub>2</sub> levels tested ( $p < 0.05$ ) (Table 5). The C : Si ratios of *P. subcurvata* at CO<sub>2</sub> levels lower than 755 ppm at 8 °C were significantly lower than at 2 °C ( $p < 0.05$ ) (Table 5). The higher temperature also significantly increased the C : Chl *a* ratios of *P. subcurvata* at all the CO<sub>2</sub> levels tested ( $p < 0.05$ ) (Table 5). Additionally, the temperature increase and CO<sub>2</sub>

concentration increase interactively decreased the C : Chl *a* ratios of *P. subcurvata* ( $p < 0.05$ ) (Table 5).

The CO<sub>2</sub> concentration increase did not affect the C : N, N : P, and C : P ratios of *P. antarctica* at either 2 °C or 8 °C. The carbon to Chl *a* ratios of *P. antarctica* were significantly higher at 1730 ppm than at all lower CO<sub>2</sub> concentrations at 2 °C. Similarly, at 8 °C the carbon to Chl *a* ratios of this species were also significantly higher at 425, 755, and 1730 ppm than at lower CO<sub>2</sub> concentrations ( $p < 0.05$ ) (Table 5), and significantly higher at 1730 ppm than at 425 and 755 ppm ( $p < 0.05$ ) (Table 5).

The warmer temperature significantly decreased the C : N ratios of *P. antarctica* at 260 and 755 ppm CO<sub>2</sub> ( $p < 0.05$ ) (Table 5), and C : P ratios also decreased at 100 and 205 ppm ( $p < 0.05$ ) (Table 5). The C : Chl *a* ratios of *P. antarctica* at CO<sub>2</sub> levels higher than 205 ppm were significantly higher at 8 °C relative to 2 °C ( $p < 0.05$ ) (Table 5). Temperature and CO<sub>2</sub> concentration increase interactively increased the C : Chl *a* ratios of *P. antarctica* ( $p < 0.05$ ) (Table 5).

The CO<sub>2</sub> concentration increase did not affect the cellular C, N, P, or Si quotas of *P. subcurvata* at 2 °C, nor the C quotas and N quotas at 8 °C. The Si quotas of *P. subcurvata* were significantly lower at 1730 ppm CO<sub>2</sub> than at 100 and 205 ppm at 8 °C ( $p < 0.05$ ) (Table 6). The cellular Chl *a* quotas of *P. subcurvata* were significantly lower at 8 °C relative to 2 °C at CO<sub>2</sub> higher than 205 ppm ( $p < 0.05$ ) (Table 6). The temperature increase significantly increased the cellu-

**Table 3.** The effects of temperature on the C quota (pmol cell<sup>-1</sup>), N quota (pmol cell<sup>-1</sup>), P quota (pmol cell<sup>-1</sup>), Si quota (pmol cell<sup>-1</sup>), and Chl *a* per cell (pg cell<sup>-1</sup>) of *P. subcurvata* and *P. antarctica*. Values represent the means and errors are the standard deviations of triplicate bottles.

	<i>P. subcurvata</i>	<i>P. antarctica</i>
<b>C quota</b>		
0 °C	1.91 ± 0.14	2.64 ± 0.34
2 °C	2.11 ± 0.19	2.49 ± 0.41
4 °C	2.15 ± 0.12	2.50 ± 0.23
6 °C	2.07 ± 0.13	2.26 ± 0.18
8 °C	2.33 ± 0.14	2.17 ± 0.22
10 °C	2.17 ± 0.13	
<b>N quota</b>		
0 °C	0.27 ± 0.03	0.39 ± 0.03
2 °C	0.29 ± 0.03	0.36 ± 0.02
4 °C	0.33 ± 0.02	0.40 ± 0.01
6 °C	0.31 ± 0.01	0.35 ± 0.02
8 °C	0.36 ± 0.05	0.34 ± 0.03
10 °C	0.33 ± 0.04	
<b>P quota</b>		
0 °C	0.02 ± 0.00	0.03 ± 0.00
2 °C	0.02 ± 0.00	0.02 ± 0.00
4 °C	0.03 ± 0.00	0.03 ± 0.01
6 °C	0.03 ± 0.00	0.02 ± 0.00
8 °C	0.03 ± 0.00	0.02 ± 0.00
10 °C	0.02 ± 0.00	
<b>Si quota</b>		
0 °C	0.23 ± 0.02	
2 °C	0.23 ± 0.06	
4 °C	0.30 ± 0.01	
6 °C	0.30 ± 0.03	
8 °C	0.34 ± 0.01	
10 °C	0.28 ± 0.04	
<b>Chl <i>a</i> per cell (pg cell<sup>-1</sup>)</b>		
0 °C	0.48 ± 0.01	0.23 ± 0.03
2 °C	0.57 ± 0.07	0.22 ± 0.02
4 °C	0.64 ± 0.01	0.20 ± 0.01
6 °C	0.68 ± 0.05	0.21 ± 0.00
8 °C	0.58 ± 0.03	0.17 ± 0.02
10 °C	0.46 ± 0.03	

lar Si quota of *P. subcurvata* at all the CO<sub>2</sub> levels tested except 1730 ppm ( $p < 0.05$ ) (Table 6). Additionally, warming and CO<sub>2</sub> concentration interactively decreased the cellular Si quotas of *P. subcurvata* ( $p < 0.05$ ) (Table 6).

**Table 4.** Comparison of the curve fitting results for maximum growth rate (d<sup>-1</sup>) and half-saturation constants ( $K_{1/2}$ ), calculated from the CO<sub>2</sub> functional response curves of *P. subcurvata* and *P. antarctica* at 2 and 8 °C. Values represent the means and errors are the standard errors from fitting.

Species	Maximum growth rates (d <sup>-1</sup> )	$K_{1/2}$ ppm CO <sub>2</sub>
<i>P. subcurvata</i>		
2 °C	0.60 ± 0.18	66.4 ± 10.39
8 °C	0.88 ± 0.02	9.8 ± 5.34
<i>P. antarctica</i>		
2 °C	0.61 ± 0.02	26.4 ± 8.23
8 °C	0.41 ± 0.02	22.1 ± 11.15

The C, N, and P quotas of *P. antarctica* were not affected by CO<sub>2</sub> increase at 2 °C, and N and P quotas were not affected by CO<sub>2</sub> increase at 8 °C either. However, the C quota of *P. antarctica* at 1730 ppm CO<sub>2</sub> was significantly higher than at CO<sub>2</sub> levels lower than 755 ppm at 8 °C ( $p < 0.05$ ) (Table 6). The Chl *a* per cell of *P. antarctica* at 1730 ppm CO<sub>2</sub> was significantly less than at lower CO<sub>2</sub> levels at both 2 and 8 °C ( $p < 0.05$ ) (Table 6). For *P. antarctica*, the values of Chl *a* per cell at 100, 205, and 755 ppm CO<sub>2</sub> at 8 °C were significantly lower relative to 2 °C ( $p < 0.05$ ) (Table 6). Temperature increase and CO<sub>2</sub> concentration increase interactively increased the C and N quotas of *P. antarctica* ( $p < 0.05$ ) (Table 6).

#### 4 Discussion

As has been documented in previous work, the diatom *P. subcurvata* and the prymnesiophyte *P. antarctica* responded differently to warming (Xu et al., 2014; Zhu et al., 2016). In the Ross Sea as elsewhere, temperature determines both phytoplankton maximum growth rates (Bissinger et al., 2008) and the upper limit of growth (Smith and Sakshaug, 1990) in a species-specific manner. Thermal functional response curves of phytoplankton typically increase in a normally distributed pattern, with growth rates increasing up to the optimum temperature range, and then declining when temperature reaches inhibitory levels (Boyd et al., 2013; Fu et al., 2014; Xu et al., 2014; Hutchins and Fu, 2017). Specific growth rates of *P. subcurvata* reached optimal levels at 8 °C, demonstrating that this species grows fastest at temperatures substantially above any temperatures found in the present-day Ross Sea. In contrast, growth rates of *P. antarctica* saturated at 2 °C. This suggests that *P. subcurvata* may be a superior competitor over *P. antarctica* in any realistically foreseeable warming scenario.

Zhu et al. (2016) found that 4 °C warming significantly promoted the growth rates of *P. subcurvata* but not *P. antarctica*.



**Table 5.** The effects of CO<sub>2</sub> on the C:N, N:P, C:P, C:Si, and C:Chl *a* ratios of *P. subcurvata* and *P. antarctica* at 2 and 8 °C. Values represent the means and errors are the standard deviations of triplicate bottles.

	<i>P. subcurvata</i>		<i>P. antarctica</i>	
	2 °C	8 °C	2 °C	8 °C
<b>C:N</b>				
100 ppm	6.6 ± 0.26	7.1 ± 0.68	7.22 ± 0.50	6.95 ± 0.35
205 ppm	6.7 ± 0.24	7.5 ± 0.32	7.74 ± 0.21	6.56 ± 1.15
260 ppm	6.7 ± 0.32	7.3 ± 0.18	8.07 ± 0.52	6.99 ± 0.27
425 ppm	6.7 ± 0.05	6.6 ± 0.05	7.21 ± 0.81	6.19 ± 0.13
755 ppm	6.8 ± 0.20	7.1 ± 0.68	7.98 ± 0.44	6.79 ± 0.22
1730 ppm	7.1 ± 0.82	7.4 ± 1.07	8.15 ± 0.48	7.05 ± 0.91
<b>N:P</b>				
100 ppm	10.4 ± 0.85	14.5 ± 2.28	16.4 ± 1.24	13.9 ± 0.20
205 ppm	10.8 ± 1.01	13.3 ± 0.42	16.6 ± 1.12	15.7 ± 2.77
260 ppm	10.3 ± 1.28	14.0 ± 0.56	14.3 ± 1.24	14.5 ± 2.38
425 ppm	11.3 ± 0.84	16.5 ± 0.28	17.1 ± 1.83	17.2 ± 1.98
755 ppm	9.9 ± 0.28	14.3 ± 1.34	14.2 ± 2.60	11.6 ± 4.11
1730 ppm	10.4 ± 1.02	15.5 ± 1.84	15.5 ± 0.56	15.1 ± 1.85
<b>C:P</b>				
100 ppm	68.6 ± 3.10	101.0 ± 6.43	117.7 ± 4.08	96.7 ± 4.86
205 ppm	72.7 ± 4.82	99.3 ± 7.05	128.2 ± 5.98	101.0 ± 1.91
260 ppm	69.1 ± 7.68	103.0 ± 4.88	115.5 ± 7.25	101.0 ± 13.04
425 ppm	76.3 ± 5.19	109.0 ± 2.20	122.3 ± 4.85	106.0 ± 11.14
755 ppm	67.2 ± 1.38	101.0 ± 5.80	113.5 ± 22.50	78.6 ± 27.09
1730 ppm	73.4 ± 1.22	114.0 ± 5.99	126.2 ± 12.10	105.0 ± 6.26
<b>C:Si</b>				
100 ppm	7.8 ± 0.80	5.6 ± 0.32		
205 ppm	7.4 ± 0.30	5.6 ± 0.24		
260 ppm	7.3 ± 0.23	6.1 ± 0.38		
425 ppm	7.5 ± 0.23	6.1 ± 0.06		
755 ppm	7.4 ± 0.66	6.3 ± 0.36		
1730 ppm	8.0 ± 0.88	7.1 ± 0.47		
<b>C:Chl <i>a</i> (µg µg<sup>-1</sup>)</b>				
100 ppm	43.6 ± 1.14	70.7 ± 5.01	160.4 ± 6.68	197.4 ± 29.35
205 ppm	45.2 ± 2.91	67.3 ± 4.42	157.5 ± 4.95	194.0 ± 17.14
260 ppm	41.6 ± 3.31	60.1 ± 9.45	138.3 ± 15.19	169.8 ± 9.20
425 ppm	37.2 ± 2.58	72.5 ± 2.35	180.2 ± 20.10	232.4 ± 20.47
755 ppm	42.2 ± 3.62	68.7 ± 6.29	167.5 ± 5.06	282.5 ± 15.30
1730 ppm	46.3 ± 2.23	85.3 ± 15.70	276.5 ± 36.57	460.3 ± 15.21

*tica*. Xu et al. (2014) found that the growth rates of another strain of *P. antarctica* (CCMP3314) decreased in a multi-variable “year 2100 cluster” condition (6 °C, 81 Pa CO<sub>2</sub>, 150 µmol photons m<sup>-2</sup> s<sup>-1</sup>) relative to the “current condition” (2 °C, 39 Pa CO<sub>2</sub>, and 50 µmol photons m<sup>-2</sup> s<sup>-1</sup>) and the “year 2060 condition” (4 °C, 61 Pa CO<sub>2</sub>, and 100 µmol photons m<sup>-2</sup> s<sup>-1</sup>). In our study, the *Q*<sub>10</sub> value of *P. subcurvata* from 0 to 4 °C was 3.11, nearly 50 % higher than the *Q*<sub>10</sub> value of *P. antarctica* across the same temperature range (2.17), and similar to the *Q*<sub>10</sub> values ob-

served for different strains of these two species in Zhu et al. (2016). Such *Q*<sub>10</sub> values that substantially exceed the canonical value of 2 are often observed in polar marine organisms (Clarke et al., 1983; Hutchins and Boyd, 2016). Our results showed that the maximal thermal limit of *P. antarctica* was reached at 10 °C, as was also observed by Buma et al. (1991), while *P. subcurvata* did not cease to grow until 14 °C. Clearly, *P. subcurvata* has a superior tolerance to higher temperature compared to *P. antarctica*.

**Table 6.** The effects of CO<sub>2</sub> on the C quota (pmol cell<sup>-1</sup>), N quota (pmol cell<sup>-1</sup>), P quota (pmol cell<sup>-1</sup>), Si quota (pmol cell<sup>-1</sup>), and Chl *a* per cell (pg cell<sup>-1</sup>) of *P. subcurvata* and *P. antarctica* at 2 and 8 °C. Values represent the means and errors are the standard deviations of triplicate bottles.

	<i>P. subcurvata</i>		<i>P. antarctica</i>	
	2 °C	8 °C	2 °C	8 °C
<b>C quota</b>				
100 ppm	2.0 ± 0.15	2.64 ± 0.06	2.57 ± 0.03	2.15 ± 0.22
205 ppm	2.1 ± 0.12	2.67 ± 0.31	2.72 ± 0.28	2.35 ± 0.19
260 ppm	1.9 ± 0.04	2.28 ± 0.18	2.51 ± 0.36	2.21 ± 0.04
425 ppm	1.8 ± 0.04	2.43 ± 0.15	2.31 ± 0.05	2.28 ± 0.46
755 ppm	2.1 ± 0.09	2.26 ± 0.05	2.47 ± 0.17	2.81 ± 0.15
1730 ppm	2.1 ± 0.30	2.47 ± 0.18	2.43 ± 0.10	2.96 ± 0.30
<b>N quota</b>				
100 ppm	0.30 ± 0.03	0.38 ± 0.04	0.36 ± 0.03	0.31 ± 0.03
205 ppm	0.30 ± 0.03	0.36 ± 0.03	0.35 ± 0.03	0.36 ± 0.06
260 ppm	0.29 ± 0.01	0.31 ± 0.02	0.31 ± 0.06	0.32 ± 0.02
425 ppm	0.27 ± 0.01	0.37 ± 0.06	0.32 ± 0.03	0.37 ± 0.05
755 ppm	0.30 ± 0.02	0.32 ± 0.03	0.31 ± 0.03	0.41 ± 0.01
1730 ppm	0.29 ± 0.05	0.34 ± 0.06	0.30 ± 0.03	0.43 ± 0.10
<b>P quota</b>				
100 ppm	0.03 ± 0.00	0.03 ± 0.00	0.02 ± 0.00	0.02 ± 0.00
205 ppm	0.03 ± 0.00	0.03 ± 0.00	0.02 ± 0.00	0.02 ± 0.00
260 ppm	0.03 ± 0.00	0.02 ± 0.00	0.02 ± 0.00	0.02 ± 0.00
425 ppm	0.02 ± 0.00	0.02 ± 0.00	0.02 ± 0.00	0.02 ± 0.01
755 ppm	0.03 ± 0.00	0.02 ± 0.00	0.02 ± 0.00	0.04 ± 0.02
1730 ppm	0.03 ± 0.00	0.02 ± 0.00	0.02 ± 0.00	0.03 ± 0.00
<b>Si quota</b>				
100 ppm	0.26 ± 0.02	0.47 ± 0.04		
205 ppm	0.28 ± 0.02	0.48 ± 0.07		
260 ppm	0.27 ± 0.01	0.37 ± 0.03		
425 ppm	0.25 ± 0.01	0.40 ± 0.04		
755 ppm	0.28 ± 0.03	0.36 ± 0.03		
1730 ppm	0.26 ± 0.01	0.35 ± 0.05		
<b>Chl <i>a</i> per cell (pg cell<sup>-1</sup>)</b>				
100 ppm	0.54 ± 0.05	0.45 ± 0.04	0.19 ± 0.01	0.13 ± 0.02
205 ppm	0.54 ± 0.04	0.48 ± 0.05	0.21 ± 0.02	0.15 ± 0.02
260 ppm	0.56 ± 0.03	0.46 ± 0.04	0.22 ± 0.04	0.16 ± 0.01
425 ppm	0.60 ± 0.04	0.40 ± 0.04	0.16 ± 0.02	0.12 ± 0.01
755 ppm	0.59 ± 0.06	0.40 ± 0.03	0.18 ± 0.01	0.12 ± 0.00
1730 ppm	0.53 ± 0.06	0.35 ± 0.05	0.11 ± 0.02	0.08 ± 0.01

The co-incubation experiment with *P. subcurvata* and *P. antarctica* at 0 and 6 °C confirmed that the diatom retained its growth advantage at the higher temperature when growing together with *P. antarctica*. Although the growth rates of the *P. subcurvata* and *Phaeocystis* cultures were not significantly different at 0 °C in unialgal cultures (Fig. 1), the diatom slightly outcompeted the prymnesiophyte even at this temperature. It is possible that there were other types of competitive interactions not related to temperature when

these two phytoplankton were grown together. For instance, the nutrient uptake and utilization strategy of *P. subcurvata* could have provided it with an advantage in the co-incubation. However, the competitive advantage enjoyed by the diatom was clearly largest at the higher temperatures, so thermal effects on competition are still evident from this experiment. Although we do not know what role (if any) competition for resources like nutrients may have played in determining the outcome of this experiment, it did demon-

strate clearly that thermal growth response trends in simple model communities are in general consistent with those seen in unialgal cultures. Xu et al. (2014) observed that the diatom *Fragilariopsis cylindrus* was dominant over *P. antarctica* under “year 2060 conditions” (4 °C, 61 Pa CO<sub>2</sub>, and 100 μmol photons m<sup>-2</sup> s<sup>-1</sup>). These experiments support the results of a Ross Sea field survey which suggested that water temperature structured the phytoplankton assemblage (Liu and Smith, 2012) and may shed light on why *P. antarctica* is often dominant in cooler waters in the springtime, while diatoms often dominate in summer (DiTullio and Smith, 1996; Arrigo et al., 1999; DiTullio et al., 2000; Liu and Smith, 2012).

Besides temperature, mixed layer depth and irradiance also likely play a role in the competition between diatoms and *P. antarctica* (Arrigo et al., 1999, 2010; Smith and Jones, 2015). Arrigo et al. (1999) observed that *P. antarctica* dominated the southern Ross Sea region with deeper mixed layers, while diatom dominated the regions with shallower mixed layer depths. The niches of these two groups of phytoplankton are difficult to define by either light or by temperature, since shallow surface stratification tends to promote both solar heating and high irradiance, while deep mixing often lowers both light and temperatures. It is worth considering whether these two phytoplankton groups are each best adapted to a different environmental matrix of both variables. This concept of different light/temperature niches for Ross Sea diatoms and *P. antarctica* is worthy of further investigation.

Our experiments used nutrient-replete conditions, which are relevant to most of the Ross Sea HNLC region throughout most of the growing season. However, major nutrients sometimes become depleted late in the season on McMurdo Sound, the origin of our culture isolates, as Fe inputs are somewhat higher in these nearshore waters (Bertrand et al., 2015). Experiments using nutrient-limited phytoplankton frequently find differing responses to CO<sub>2</sub> and temperature compared to those of nutrient-replete cells, including sometimes enhanced effects of these global change factors on elemental ratios (Taucher et al., 2015; Sala et al., 2016). Our experiments under high-nutrient, Fe-replete conditions thus are likely to best predict possible biological effects of future high CO<sub>2</sub> and temperature during the first half or more of the Ross Sea growing season.

Temperature change affected the C : P, N : P, and C : Si ratios of *P. subcurvata*, due to the combined effects of the different responses of cellular C, P, and Si quotas. The C : P and N : P ratios of *P. subcurvata* increased at the two highest temperatures tested. This might be due to an increase in protein translation efficiency and a corresponding decrease in phosphate-rich ribosomes with warming, which can result in a decreased cellular P requirement per unit of carbon in marine phytoplankton (Toseland et al., 2013). Similarly lowered P quotas at higher temperatures have been documented in other studies as well (Xu et al., 2014; Boyd et

al., 2015; Hutchins and Boyd, 2016). This result suggests that the amount of carbon exported per unit phosphorus by *P. subcurvata* (and perhaps other diatoms) in the Ross Sea may increase as temperature increases in the future (Toseland et al., 2013).

In contrast, the decreasing trend of C : Si ratios in *P. subcurvata* appears to be largely due to higher cellular Si quotas at temperatures of 4 °C and above. Although the physiological reason(s) for increased silicification with warming are currently not understood, this trend also may have biogeochemical consequences. This decrease in cellular C : Si ratios at higher temperature may tend to enhance Si export, with the qualification that biogenic Si remineralization rates also increase with temperature (Ragueneau et al., 2000) and thus could potentially offset this trend.

Previous studies have shown that nutrient drawdown by diatoms and *P. antarctica* is different, due to differing elemental ratios of these two groups (Arrigo et al., 1999; Smith et al., 2014a; Xu et al., 2014). Our results generally corresponded to this trend, as the N : P ratios of *P. antarctica* were higher than *P. subcurvata* at 2, 6, and 8 °C and C : P ratios of *P. antarctica* were higher than *P. subcurvata* at 6 and 8 ( $p < 0.05$ ) (Fig. 2). Although elemental ratios of the prymnesiophyte were largely unaffected by temperature, a predicted increase in diatom and decrease in *P. antarctica* contributions to phytoplankton production caused by warming will likely change nutrient export ratios (Smith et al., 2014a, b). It is possible that N and C export per unit P may decrease with a phytoplankton community shift from *P. antarctica* dominance to diatom dominance (Arrigo et al., 1999; Smith et al., 2014a, b; Xu et al., 2014). However, food web effects may compensate for the effects of temperature on biogeochemical cycles, as diatoms are a preferred food source for zooplankton grazers, compared to *Phaeocystis* (Knox, 1994; Caron et al., 2000; Haberman et al., 2003).

Our results showed that the growth rates of both *P. subcurvata* and *P. antarctica* exhibited moderate limitation by CO<sub>2</sub> levels lower than ~425 ppm at both 2 and 8 °C; this observation is significant, since during the intense Ross Sea summertime phytoplankton bloom pCO<sub>2</sub> can sometimes drop to very low levels (Tagliabue and Arrigo, 2016). However, at CO<sub>2</sub> concentrations beyond current atmospheric levels of ~400 ppm, growth rates of *P. subcurvata* or *P. antarctica* were CO<sub>2</sub>-saturated. Although a general model prediction suggests that an atmospheric CO<sub>2</sub> increase from current levels to 700 ppm could increase the growth of marine phytoplankton by 40 % (Schippers et al., 2004), our results instead correspond to previous studies which showed negligible effects of elevated CO<sub>2</sub> on various groups of phytoplankton (Goldman, 1999; Fu et al., 2007; Hutchins and Fu 2017). In particular, Trimborn et al. (2013) found that increasing CO<sub>2</sub> had no effect on growth rates of Southern Ocean isolates of *P. subcurvata* and *P. antarctica*. The minimal effects of changing CO<sub>2</sub> levels on many phytoplankton groups have been suggested to be due to efficient car-

bon concentrating mechanisms (CCMs) that allow them to avoid CO<sub>2</sub> limitation at low *p*CO<sub>2</sub> levels (Burkhardt et al., 2001; Fu et al., 2007; Tortell et al., 2008). For instance, both *P. subcurvata* and *P. antarctica* have been shown to strongly downregulate activity of the important CCM enzyme carbonic anhydrase as CO<sub>2</sub> increases (Trimborn et al., 2013). Clearly, though, for our two species their CCM activity was not sufficient to completely compensate for carbon limitation at low *p*CO<sub>2</sub> levels. Although speculative, it is possible that *P. antarctica* could have an ability to subsidize growth at very low CO<sub>2</sub> levels through oxidation of organic carbon from the colony mucilage. Our results also showed that very high CO<sub>2</sub> (1730 ppm) significantly reduced the growth rate of *P. antarctica* relative to 425 and 755 ppm at 2 °C. This inhibitory effect might be due to the significantly lower pH at 1730 ppm (~7.4), which could entail expenditures of additional energy to maintain pH homeostasis within cells. Similar negative effects of high CO<sub>2</sub> have been observed on *P. antarctica* in natural communities (Hancock et al., 2017), as well as on a mixed Antarctic microbial assemblage (Davidson et al., 2016).

Warming from 2 to 8 °C had a significant interactive effect with CO<sub>2</sub> concentration in *P. subcurvata*, as maximum growth rates were higher and the half-saturation constant ( $K_{1/2}$ ) for growth was much lower at the warmer temperature. In contrast, warming decreased the maximal growth rates of *P. antarctica* over the range of CO<sub>2</sub> concentrations tested, and failed to change its  $K_{1/2}$  for growth. The decreased CO<sub>2</sub>  $K_{1/2}$  of *P. subcurvata* at high temperature might confer a future additional competitive advantage over *P. antarctica* in the late growing season, when *p*CO<sub>2</sub> can be low (Tagliabue and Arrigo, 2016) and temperatures higher, although temperatures are generally never as high as 8 °C in the current Ross Sea (Liu and Smith, 2012). The interactive effects of temperature and CO<sub>2</sub> on *P. subcurvata* might be due to elevated enzyme and protein translation efficiencies at higher temperature, which may decrease the CO<sub>2</sub> requirement of the Calvin cycle and facilitate allocation of fixed carbon to growth (Toseland et al., 2013; Hutchins and Boyd, 2016). On the other hand, 8 °C is clearly close to the upper thermal limit of *P. antarctica*, suggesting that its biochemical efficiencies decline rapidly above this temperature. The  $K_{1/2}$  of *P. antarctica* for CO<sub>2</sub> was, however, significantly lower than that of *P. subcurvata* at 2 °C, which may be advantageous to the prymnesiophyte when water temperatures are low in the spring.

The effects of *p*CO<sub>2</sub> variation on the elemental ratios of *P. subcurvata* and *P. antarctica* were minimal relative to those of temperature increase. Previous research on the effects of CO<sub>2</sub> on the elemental ratios of phytoplankton has shown that the elemental composition of phytoplankton may change with CO<sub>2</sub> availability (Burkhardt et al., 1999; Fu et al., 2007, 2008; Tew et al., 2014; reviewed in Hutchins et al., 2009). Hoogstraten et al. (2012) found that CO<sub>2</sub> concentration change did not change the cellular POC, PON, C : N

ratios, or POC to Chl *a* ratios of the temperate species *Phaeocystis globosa*. In contrast, Reinfelder (2014) observed that the N and P quotas of several diatoms decreased with increasing CO<sub>2</sub> and led to increased C : N, N : P, and C : P ratios. King et al. (2015) found that high CO<sub>2</sub> could increase, decrease or not affect the C : P and N : P ratios of several different phytoplankton species. Our results resemble those of studies with other phytoplankton that found that the effects of CO<sub>2</sub> concentration can be negligible on C : N, N : P, or C : P ratios (Fu et al., 2007; Hutchins et al., 2009; Hoogstraten et al., 2012; King et al., 2015), including incubation studies with Antarctic communities (Deppeler et al., 2017). It is possible that such contrasting effects of CO<sub>2</sub> concentration on the elemental ratios of phytoplankton are due to species-specific differences in biochemical composition (e.g., proteins are enriched with N and membranes with P relative to other cellular components) or to differences in experimental design, which can make intercomparisons problematic (Hutchins and Fu, 2017).

In contrast to C : N : P ratios, we observed that the C : Si ratios of *P. subcurvata* were significantly higher at 1730 ppm compared to almost all of the lower CO<sub>2</sub> levels. This increase in C : Si ratios was due to a decrease in cellular Si quotas at 1730 ppm CO<sub>2</sub>. Milligan et al. (2004) observed that the silica dissolution rates of a temperate diatom increased significantly in high CO<sub>2</sub> relative to in low-CO<sub>2</sub> cultures. Tatters et al. (2012) found a similar trend in the temperate toxic diatom *Pseudo-nitzschia fraudulenta*, in which cellular C : Si ratios were higher at 765 ppm than at 200 ppm CO<sub>2</sub>. This suggests that future increases in diatom silicification at elevated temperature could partially or wholly offset the decreased silicification and higher dissolution rates of silica observed high CO<sub>2</sub> (above); to fully predict net trends, further interactive experiments focusing on silicification as a function across a range of both temperature and *p*CO<sub>2</sub> are needed.

In conclusion, our results indicate that *P. subcurvata* from the Ross Sea is better adapted to higher temperature than is *P. antarctica*. Diatoms are a diverse group, but if their general thermal response is similar to that of this *Pseudo-nitzschia* species, they may thrive under future global warming scenarios, while the relative dominance of *P. antarctica* in this region may wane. In contrast, another recent study has suggested that warming might indirectly favor *P. antarctica* springtime dominance by leading to large areas of open water at a time when incident light penetration is low and mixed layers are still relatively deep (Ryan-Keogh et al., 2017). Because of the differences in elemental ratios in the two groups, ecological shifts that favor diatoms may significantly increase the export of phosphorus and silicon relative to carbon and nitrogen, while increased *P. antarctica* dominance will increase carbon export relative to nutrient fluxes, as well as enhancing the organic sulfur cycle. Our conclusions must be qualified as they were obtained using Fe-replete culture conditions, similar to conditions often found early in the growing season in McMurdo Sound. However, Fe limitation

generally prevails later in the season here, and elsewhere in the offshore Ross Sea. Irradiance is an additional key environmental factor to consider in both the present and future in this region (Smith and Jones, 2015). Thus, in addition to warming and CO<sub>2</sub> increases, the interactive effects of light and Fe with these two factors should also be considered (Xu et al., 2014; Boyd et al., 2015; Hutchins and Boyd, 2016; Hutchins and Fu, 2017). Considering the differences between the responses of the diatom and *P. antarctica* to warming and ocean acidification seen here, as well to warming and Fe in previous work (Zhu et al., 2016), models attempting to predict future changes in community structure and primary production in the Ross Sea polynya may need to realistically incorporate a complex network of interacting global change variables.

**Data availability.** The data have been submitted to the Biological and Chemical Oceanography Data Management Office at Woods Hole, MA, USA. Until they become available online, please contact the corresponding author with data requests.

**Author contributions.** ZZ, FXF, and DAH designed the experiments; ZZ, PQ, and JG carried them out; and ZZ and DAH wrote the manuscript.

**Competing interests.** The authors declare that they have no conflict of interest.

**Acknowledgements.** We want to thank Kai Xu for isolating all these phytoplankton strains. Support for this research was provided by National Science Foundation grant ANT 1043748 to D. A. Hutchins.

Edited by: Koji Suzuki

Reviewed by: Andrew McMinn, Katherina Petrou, and three anonymous referees

## References

- Arrigo, K. R., Robinson, D. H., Worthen, D. L., Dunbar, R. B., DiTullio, G. R., Van Woert, M., and Lizotte, M. P.: Phytoplankton community structure and the drawdown of nutrients and CO<sub>2</sub> in the Southern Ocean, *Science*, 283, 365–367, 1999.
- Arrigo K. R., DiTullio G. R., Dunbar R. B., Robinson D. H., Van Woert M., Worthen D. L., and Lizotte, M. P.: Phytoplankton taxonomic variability in nutrient utilization and primary production in the Ross Sea, *J. Geophys. Res.-Oceans*, 105, 8827–8846, 2000.
- Arrigo, K. R., van Dijken, G. L., and Bushinsky, S.: Primary production in the Southern Ocean, 1997–2006, *J. Geophys. Res.*, 113, C08004, <https://doi.org/10.1029/2007JC004551>, 2008.
- Arrigo, K. R., Mills, M. M., Kropuenske, L. R., van Dijken, G. L., Alderkamp, A. C., and Robinson, D. H.: Photophysiology in two major Southern Ocean phytoplankton taxa: photosynthesis and growth of *Phaeocystis antarctica* and *Fragilariopsis cylindrus* under different irradiance levels, *Integr. Comp. Biol.*, 50, 950–966, 2010.
- Bertrand, E. M., McCrow, J. P., Zheng, H., Moustafa, A., McQuaid, J., Delmont, T., Post, A., Sipler, R., Spackeen, J., Xu, K., Bronk, D., Hutchins, D. A., and Allen, A. E.: Phytoplankton-bacterial interactions mediate micronutrient colimitation in the Southern Ocean, *P. Natl. Acad. Sci. USA*, 112, 9938–9943, <https://doi.org/10.1073/pnas.1501615112>, 2015.
- Bissinger, J. E., Montagnes, D. J., Sharples, J., and Atkinson, D.: Predicting marine phytoplankton maximum growth rates from temperature: Improving on the Eppley curve using quantile regression, *Limnol. Oceanogr.*, 53, 487–493, <https://doi.org/10.4319/lo.2008.53.2.0487>, 2008.
- Boyd, P. W., Rynearson, T. A., Armstrong, E. A., Fu, F., Hayashi, K., Hu, Z., Hutchins, D. A., Kudela, R. M., Litchman, E., Mulholland, M. R., and Passow, U.: Marine phytoplankton temperature versus growth responses from polar to tropical waters—outcome of a scientific community-wide study, *PLoS One*, 8, <https://doi.org/10.1371/journal.pone.0063091>, 2013.
- Boyd, P. W., Dillingham, P. W., McGraw, C. M., Armstrong, E. A., Cornwall, C. E., Feng, Y. Y., Hurd, C. L., Gault-Ringold, M., Roleda, M. Y., Timmins-Schiffman, E., and Nunn, B. L.: Physiological responses of a Southern Ocean diatom to complex future ocean conditions, *Nat. Clim. Change*, 6, 207–213, 2015.
- Boyd, P. W., Watson, A. J., Law, C. S., Abraham, E. R., Trull, T., Murdoch, R., Bakker, D. C., Bowie, A. R., Buesseler, K. O., Chang, H., and Charette, M.: A mesoscale phytoplankton bloom in the polar Southern Ocean stimulated by iron fertilization, *Nature*, 407, 695–702, 2000.
- Buma, A. G. J., Bano, N., Veldhuis, M. J. W., and Kraay, G. W.: Comparison of the pigmentation of two strains of the prymnesiophyte *Phaeocystis* sp., *Neth. J. Sea Res.*, 27, 173–182, 1991.
- Burkhardt, S., Zondervan, I., and Riebesell, U.: Effect of CO<sub>2</sub> concentration on C:N:P ratio in marine phytoplankton: A species comparison, *Limnol. Oceanogr.*, 44, 683–690, 1999.
- Burkhardt, S., Amoroso, G., Riebesell, U., and Sültemeyer, D.: CO<sub>2</sub> and HCO<sub>3</sub><sup>-</sup> uptake in marine diatoms acclimated to different CO<sub>2</sub> concentrations, *Limnol. Oceanogr.*, 46, 1378–1391, 2001.
- Caron, D. A., Dennett, M. R., Lonsdale, D. J., Moran, D. M., and Shalapyonok, L.: Microzooplankton herbivory in the Ross sea, Antarctica, *Deep-Sea Res. Pt. II*, 47, 3249–3272, 2000.
- Chau-Berlinck, J. G., Monteiro, L. H. A., Navas, C. A., and Bicudo, J. E. P.: Temperature effects on energy metabolism: a dynamic system analysis, *P. Roy. Soc. Lond. B-Bio.*, 269, 15–19, 2002.
- Clarke, A.: Life in cold water: the physiological ecology of polar marine ectotherms, *Oceanogr. Mar. Biol.*, 21, 341–453, 1983.
- Coale, K. H., Johnson, K. S., Chavez, F. P., Buesseler, K. O., Barber, R. T., Brzezinski, M. A., Cochlan, W. P., Millero, F. J., Falkowski, P. G., Bauer, J. E., and Wanninkhof, R. H.: Southern Ocean iron enrichment experiment: carbon cycling in high- and low-Si waters, *Science*, 304, 408–414, 2004.
- Davidson, A. T., McKinlay, J., Westwood, K., Thompson, P. G., van den Enden, R., de Salas, M., Wright, S., Johnson, R., and Berry, K.: Enhanced CO<sub>2</sub> concentrations change the structure of

- Antarctic marine microbial communities, *Mar. Ecol.-Prog. Ser.*, 552, 92–113, 2016.
- Deppeler, S., Petrou, K., Schulz, K. G., Westwood, K., Pearce, I., McKinlay, J., and Davidson, A.: Ocean acidification of a coastal Antarctic marine microbial community reveals a critical threshold for CO<sub>2</sub> tolerance in phytoplankton productivity, *Biogeosciences Discuss.*, <https://doi.org/10.5194/bg-2017-226>, in review, 2017.
- DiTullio, G. R. and Smith, W. O.: Spatial patterns in phytoplankton biomass and pigment distributions in the Ross Sea, *J. Geophys. Res.-Oceans*, 101, 18467–18477, 1996.
- DiTullio, G. R., Grebmeier, J. M., Arrigo, K. R., Lizotte, M. P., Robinson, D. H., Leventer, A., Barry, J. P., VanWoert, M. L., and Dunbar, R. B.: Rapid and early export of *Phaeocystis antarctica* blooms in the Ross Sea, Antarctica, *Nature*, 404, 595–598, 2000.
- El-Sabaawi, R. and Harrison, P. J.: Interactive effects of irradiance and temperature on the photosynthetic physiology of the pennate diatom *Pseudo-nitzschia Granii* (Bacillariophyceae) from the northeast Subarctic Pacific, *J. Phycol.*, 42, 778–785, 2006.
- Fabry, V. J.: Marine calcifiers in a high-CO<sub>2</sub> ocean, *Science*, 320, 1020–1022, 2008.
- Fu, F. X., Warner, M. E., Zhang, Y., Feng, Y., and Hutchins, D. A.: Effects of increased temperature and CO<sub>2</sub> on photosynthesis, growth, and elemental ratios in marine *Synechococcus* and *Prochlorococcus* (cyanobacteria), *J. Phycol.*, 43, 485–496, 2007.
- Fu, F. X., Zhang, Y., Warner, M. E., Feng, Y., Sun, J., and Hutchins, D. A.: A comparison of future increased CO<sub>2</sub> and temperature effects on sympatric *Heterosigma akashiwo* and *Prorocentrum minimum*, *Harmful Algae*, 7, 76–90, 2008.
- Fu, F. X., Yu, E., Garcia, N. S., Gale, J., Luo, Y., Webb, E. A., and Hutchins, D. A.: Differing responses of marine N<sub>2</sub> fixers to warming and consequences for future diazotroph community structure, *Aquat. Microb. Ecol.*, 72, 33–46, 2014.
- Gille, S. T.: Warming of the Southern Ocean since the 1950s, *Science*, 295, 1275–1277, 2002.
- Goldman, J. C.: Inorganic carbon availability and the growth of large marine diatoms, *Mar. Ecol.-Prog. Ser.*, 180, 81–91, 1999.
- Haberman, K. L., Ross, R. M., and Quetin, L. B.: Diet of the Antarctic krill (*Euphausia superba* Dana): II. Selective grazing in mixed phytoplankton assemblages, *J. Exper. Mar. Biol. Ecol.*, 283, 97–113, 2003.
- Hancock, A. M., Davidson, A. T., McKinlay, J., McMinn, A., Schulz, K., and van den Enden, R. L.: Ocean acidification changes the structure of an Antarctic coastal protistan community, *Biogeosciences Discuss.*, <https://doi.org/10.5194/bg-2017-224>, in review, 2017.
- Hoogstraten, A., Peters, M., Timmermans, K. R., and de Baar, H. J. W.: Combined effects of inorganic carbon and light on *Phaeocystis globosa* Scherffel (Prymnesiophyceae), *Biogeosciences*, 9, 1885–1896, <https://doi.org/10.5194/bg-9-1885-2012>, 2012.
- Hutchins, D. A., Mulholland, M. R., and Fu, F. X.: Nutrient cycles and marine microbes in a CO<sub>2</sub>-enriched ocean, *Oceanography*, 22, 128–145, 2009.
- Hutchins, D. A. and Boyd, P. W.: Marine phytoplankton and the changing ocean iron cycle, *Nat. Clim. Change*, 6, 1071–1079, 2016.
- Hutchins, D. A. and Fu, F. X.: Microorganisms and ocean global change, *Nat. Microbiol.*, 2, 17508, [doi:10.1038/nmicrobiol.2017.58](https://doi.org/10.1038/nmicrobiol.2017.58), 2017.
- Hutchins, D. A., Sedwick, P. N., DiTullio, G. R., Boyd, P. W., Queguiner, B., Griffiths, F. B., and Crossley, C.: Control of phytoplankton growth by iron and silicic acid availability in the subantarctic Southern Ocean: Experimental results from the SAZ Project, *J. Geophys. Res.-Oceans*, 106, 31559–31572, 2001.
- IPCC: Climate Change 2014: Impacts, Adaptation, and Vulnerability. Part A: Global and Sectoral Aspects. Contribution of Working Group II to the Fifth Assessment Report of the Intergovernmental Panel on Climate Change, 2014.
- King, A. L., Sanudo-Wilhelmy, S. A., Leblanc, K., Hutchins, D. A., and Fu, F. X.: CO<sub>2</sub> and vitamin B12 interactions determine bioactive trace metal requirements of a subarctic Pacific diatom, *The ISME J.*, 5, 1388–1396, 2011.
- King, A. L., Jenkins, B. D., Wallace, J. R., Liu, Y., Wikfors, G. H., Milke, L. M., and Meseck, S. L.: Effects of CO<sub>2</sub> on growth rate, C:N:P, and fatty acid composition of seven marine phytoplankton species, *Mar. Ecol.-Prog. Ser.*, 537, 59–69, 2015.
- Knox, G. A.: The Biology of the Southern Ocean, Cambridge University Press, New York, USA, 1994.
- Liu, X. and Smith, W. O.: Physiochemical controls on phytoplankton distributions in the Ross Sea, Antarctica, *J. Mar. Sys.*, 94, 135–144, 2012.
- Martin, J. H., Gordon, R. M., and Fitzwater, S. E.: Iron in Antarctic waters, *Nature*, 345, 156–158, 1990.
- Meredith, M. P. and King, J. C.: Rapid climate change in the ocean west of the Antarctic Peninsula during the second half of the 20th century, *Geophys. Res. Lett.*, 32, L19604, <https://doi.org/10.1029/2005GL024042>, 2005.
- Milligan, A. J., Varela, D. E., Brzezinski, M. A., and Morel, F. M.: Dynamics of silicon metabolism and silicon isotopic discrimination in a marine diatom as a function of pCO<sub>2</sub>, *Lim. Oceanogr.*, 49, 322–329, 2004.
- Orr, J. C., Fabry, V. J., Aumont, O., Bopp, L., Doney, S. C., Feely, R. A., Gnanadesikan, A., Gruber, N., Ishida, A., Joos, F., and Key, R. M.: Anthropogenic ocean acidification over the twenty-first century and its impact on calcifying organisms, *Nature*, 437, 681–686, 2005.
- Paasche, E.: Silicon and the ecology of marine plankton diatoms II, Silicate-uptake kinetics in five diatom species, *Mar. Biol.*, 19, 262–269, 1973.
- Ragueneau, O., Tréguer, P., Leynaert, A., Anderson, R. F., Brzezinski, M. A., DeMaster, D. J., Fischer, G., Francois, R., and Heinze, C.: A review of the Si cycle in the modern ocean: recent progress and missing gaps in the application of biogenic opal as a paleo-productivity proxy, *Glob. Planet. Change*, 26, 317–365, 2000.
- Reinfeldt, J. R.: Carbon dioxide regulation of nitrogen and phosphorus in four species of marine phytoplankton, *Mar. Ecol.-Prog. Ser.*, 466, 57–67, 2012.
- Pierrot, D., Lewis, E., and Wallace, D. W. R.: MS Excel program developed for CO<sub>2</sub> system calculations. ORNL/CDIAC-105a. Carbon Dioxide Information Analysis Center, Oak Ridge National Laboratory, US Department of Energy, Oak Ridge, Tennessee, 2006.
- Rose, J. M., Feng, Y., DiTullio, G. R., Dunbar, R. B., Hare, C. E., Lee, P. A., Lohan, M., Long, M., W. O. Smith Jr., Sohst, B., Tozzi, S., Zhang, Y., and Hutchins, D. A.: Synergistic effects of iron and temperature on Antarctic phytoplankton and microzooplankton assemblages, *Biogeosciences*, 6, 3131–3147, <https://doi.org/10.5194/bg-6-3131-2009>, 2009.

- Ryan-Keogh, T. J., DeLizo, L. M., Smith, W. O. Jr., Smith, Sedwick, P. N., McGillicuddy, D. J., Jr., Moore, C. M., and Bibby, T. S.: Temporal progression of photosynthetic-strategy in phytoplankton in the Ross Sea, Antarctica, *J. Mar. Sys.*, 166, 87–96, <https://doi.org/10.1016/j.jmarsys.2016.08.014>, 2017.
- Sala, M. M., Aparicio, F. L., Balague, V., Boras, J. A., Borrull, E., Cardelus, C., Cros, L., Gomes, A., Lopez-Sanz, A., Malits, A., Martinez, R. A., Mestre, M., Movilla, J., Sarmiento, H., Vazquez-Dominguez, E., Vaque, D., Pinhassi, J., Calbet, A., Calvo, E., Gasol, J. M., Pelejero, C., and Marrase, C.: Contrasting effects of ocean acidification on the microbial food web under different trophic conditions, *ICES J. Mar. Sci.*, 73, 670–679, 2016.
- Sarmiento, J. L., Hughes, T. M., Stouffer, R. J., and Manabe, S.: Simulated response of the ocean carbon cycle to anthropogenic climate warming, *Nature*, 393, 245–249, 1998.
- Schippers, P., Lüring, M., and Scheffer, M.: Increase of atmospheric CO<sub>2</sub> promotes phytoplankton productivity, *Ecol. Lett.*, 7, 446–451, 2004.
- Schoemann, V., Becquevort, S., Stefels, J., Rousseau, V., and Lancelot, C.: *Phaeocystis* blooms in the global ocean and their controlling mechanisms: a review, *J. Sea. Res.*, 53, 43–66, 2005.
- Smith Jr., W. O. and Sakshaug, E.: Polar Phytoplankton, edited by: Smith, W. O., Polar Oceanography, Chemistry, Biology and Geology, Academic Press, Massachusetts, USA, eBook ISBN: 9780080925950, 1990.
- Sedwick, P. N., DiTullio, G. R., and Mackey, D. J.: Iron and manganese in the Ross Sea, Antarctica: Seasonal iron limitation in Antarctic shelf waters, *J. Geophys. Res.-Oceans*, 105, 11321–11336, 2000.
- Sedwick, P. N., Marsay, C. M., Sohst, B. M., Aguilar-Islas, A. M., Lohan, M. C., Long, M. C., Arrigo, K. R., Dunbar, R. B., Saito, M. A., Smith, W. O., and DiTullio, G. R.: Early season depletion of dissolved iron in the Ross Sea polynya: Implications for iron dynamics on the Antarctic continental shelf, *J. Geophys. Res.-Oceans*, 116, C12019, <https://doi.org/10.1029/2010JC006553>, 2011.
- Smith, W. O., Ainley, D. G., Arrigo, K. R., and Dinniman, M. S.: The oceanography and ecology of the Ross Sea., *Annu. Rev. Mar. Sci.*, 6, 469–487, 2014a.
- Smith, W. O., Dinniman, M. S., Hofmann, E. E., and Klinck, J. M.: The effects of changing winds and temperatures on the oceanography of the Ross Sea in the 21st century, *Geophys. Res. Lett.*, 41, 1624–1631, 2014b.
- Smith, W. O. Jr. and Jones, R. M.: Vertical mixing, critical depths, and phytoplankton growth in the Ross Sea, *ICES J. Mar. Sci.*, 72, 1952–1960, 2015.
- Smith, W. O., Marra, J., Hiscock, M. R., and Barber, R. T.: The seasonal cycle of phytoplankton biomass and primary productivity in the Ross Sea, Antarctica, *Deep-Sea Res. Pt. II*, 47, 3119–3140, 2000.
- Tagliabue, A. and Arrigo, K. R.: Decadal trends in air-sea CO<sub>2</sub> exchange in the Ross Sea (Antarctica), *Geophys. Res. Lett.*, 43, 5271–5278, 2016.
- Takeda, S.: Influence of iron availability on nutrient consumption ratio of diatoms in oceanic waters, *Nature*, 393, 774–777, 1998.
- Tatters, A. O., Fu, F. X., and Hutchins, D. A.: High CO<sub>2</sub> and silicate limitation synergistically increase the toxicity of *Pseudo-nitzshia fraudulenta*, *PLoS ONE*, 7, <https://doi.org/10.1371/journal.pone.0032116>, 2012.
- Taucher, J., Jones, J., James, A., Brzezinski, M. A., Carlson, C. A., Riebesell, U., and Passow, U. Combined effects of CO<sub>2</sub> and temperature on carbon uptake and partitioning by the marine diatoms *Thalassiosira weissflogii* and *Dactyliosolen fragilissimus*, *Limnol. Oceanogr.*, 60, 901–919, 2015.
- Tew, K. S., Kao, Y. C., Ko, F. C., Kuo, J., Meng, P. J., Liu, P. J., and Glover, D. C.: Effects of elevated CO<sub>2</sub> and temperature on the growth, elemental composition, and cell size of two marine diatoms: potential implications of global climate change, *Hydrobiologia*, 741, 79–87, 2014.
- Thomas, M. K., Kremer, C. T., Klausmeier, C. A., and Litchman, E.: A global pattern of thermal adaptation in marine phytoplankton, *Science*, 338, 1085–1088, 2012.
- Tortell, P. D., Payne, C., Gueguen, C., Li, Y., Strzepek, R. F., Boyd, P. W., and Rost, B.: Uptake and assimilation of inorganic carbon by Southern Ocean phytoplankton, *Limnol. Oceanogr.*, 53, 1266–1278, 2008.
- Toseland, A. D. S. J., Daines, S. J., Clark, J. R., Kirkham, A., Strauss, J., Uhlig, C., Lenton, T. M., Valentin, K., Pearson, G. A., Moulton, V., and Mock, T.: The impact of temperature on marine phytoplankton resource allocation and metabolism, *Nat. Clim. Change*, 3, 979–984, 2013.
- Trimborn, S., Brenneis, T., Sweet, E., and Rost, B.: Sensitivity of Antarctic phytoplankton species to ocean acidification: Growth, carbon acquisition, and species interaction, *Limnol. Oceanogr.*, 58, 997–1007, 2013.
- Wang, Y., Smith, W. O., Wang, X., and Li, S.: Subtle biological responses to increased CO<sub>2</sub> concentrations by *Phaeocystis globosa* Scherffel, a harmful algal bloom species, *Geophys. Res. Lett.*, 37, L09604, <https://doi.org/10.1029/2010GL042666>, 2010.
- Xu, K., Fu, F. X., and Hutchins, D. A.: Comparative responses of two dominant Antarctic phytoplankton taxa to interactions between ocean acidification, warming, irradiance, and iron availability, *Limnol. Oceanogr.*, 59, 1919–1931, 2014.
- Zhu, Z., Xu, K., Fu, F., Spackeen, J. L., Bronk, D. A., and Hutchins, D. A.: A comparative study of iron and temperature interactive effects on diatoms and *Phaeocystis antarctica* from the Ross Sea, Antarctica, *Mar. Ecol.-Prog. Ser.*, 550, 39–51, 2016.